JOURNAL OF COMPUTATIONAL PHYSICS **124,** 55–70 (1996)
ARTICLE NO. 0044

Numerical Computations of a Nearly Singular Nonlinear Equation: Weakly Nonlocal Bound States of Solitons for the Fifth-Order Korteweg–deVries Equation

JOHN P. BOYD*

Department of Atmospheric, Oceanic & Space Science, University of Michigan, 2455 Hayward Avenue, Ann Arbor, Michigan 48109

Received September 24, 1993; revised March 2, 1995

We numerically calculate bions, which are bound states of two solitary waves which travel together as a single coherent structure with a fixed peak-to-peak separation, for the fifth-order Korteweg–deVries equation. R. H. J. Grimshaw and B. A. Malomed (*J. Phys. A* **26** (1993), 4087–4091) predicted such bions using perturbation theory. We find that the nearly singular quasi-translational eigenmode which is the heart of the theory is also numerically important in the sense that later iterations are approximately proportional to this eigenmode. However, the near-singularity does not create any serious problems for our Fourier pseudospectral/Newton–Kantorovich/pseudoarclength continuation algorithms. This type of theory for weakly overlapping solitary waves has been previously developed by Gorshkov, Ostrovskii, Papko, and others. However, Grimshaw and Malomed's work and our own are the first on bions which are "weakly nonlocal," that is, decay for large $|x|$ to small amplitude oscillations rather than to zero. Our numerical calculations confirm the main assertions of Grimshaw and Malomed. However, there are other features, such as a complicated branch structure with multiple turning points and the existence of bions with narrow peak-to-peak separation, which are not predicted by the theory.

1. INTRODUCTION

Grimshaw and Malomed [1] predicted bound states of solitary waves for the fifth–order Korteweg–deVries (FKdV) equation

$$u_t + uu_x + u_{xxx} + u_{xxxxx} = 0, \tag{1.1}$$

where the subscripts denote differentiation with respect to the indicated coordinate. In most of the many physical and engineering problems where the ordinary KdV equation is a model for waves which are both weakly nonlinear and weakly dispersive, its fifth order generalization (1.1) is also applicable, specifically in those parameter regimes where the coefficient of the third derivative is small. The next order in the linear dispersion relation (fifth derivative) is then as important as the third derivative. It is then necessary to replace the KdV equation by its generalization; rescaling the variables gives the canonical form (1.1). There is one crucial distinction which cannot be scaled away, which is the *relative sign* of the third and fifth derivative terms. When the signs are opposite, the solitary waves decay to zero as $|x| \Rightarrow 0$. When the signs are the same, as here, the solitary waves are "weakly nonlocal" in the sense that the soliton is a *fusion* of a *single large peak* which travels, locked in phase, with a *small amplitude oscillation* which fills all of space. "Nonlocal" means that the solitary wave has nonzero amplitude even infinitely far from the large amplitude "core" of the soliton; "weakly" means that the amplitude of these "far field oscillations" or oscillatory "wings" is exponentially small in $1/\varepsilon$, where the parameter ε measures the amplitude of the core [6–9].

Grimshaw and Malomed used the perturbation methods developed by Gorshkov and Ostrovskii [2, 3] and others. Bound state solitons *per se* are not a novelty [4, 5], but the work of Grimshaw and Malomed [1] seems to be the first to treat a fusion of so-called "weakly nonlocal" solitary waves.

In this work, we have extended the Grimshaw–Malomed study through numerical computations. Our physical goal is to demonstrate that the predicted bound states actually exist and verify that peak-to-peak distances are quantized, i.e., restricted to a discrete set of values for a given amplitude. Our numerical goal is to understand how the perturbation theory is reflected in the algorithms, particularly by the near-singularity and quantization conditions which are central in the Grimshaw–Malomed analysis.

Figure 1 illustrates four different "bions" of the same amplitude. Each bion is a bound state of two ordinary, one-humped solitary waves. The large peaks are the solitons—more precisely, the "cores" of the solitons. The small oscillations are the "wings" or "far field oscillations"

* Email: jpboyd@engin.umich.edu. World-Wide Web Homepage: http://www-personal.engin.umich.edu:/~jpboyd/.

0021-9991/96 $18.00

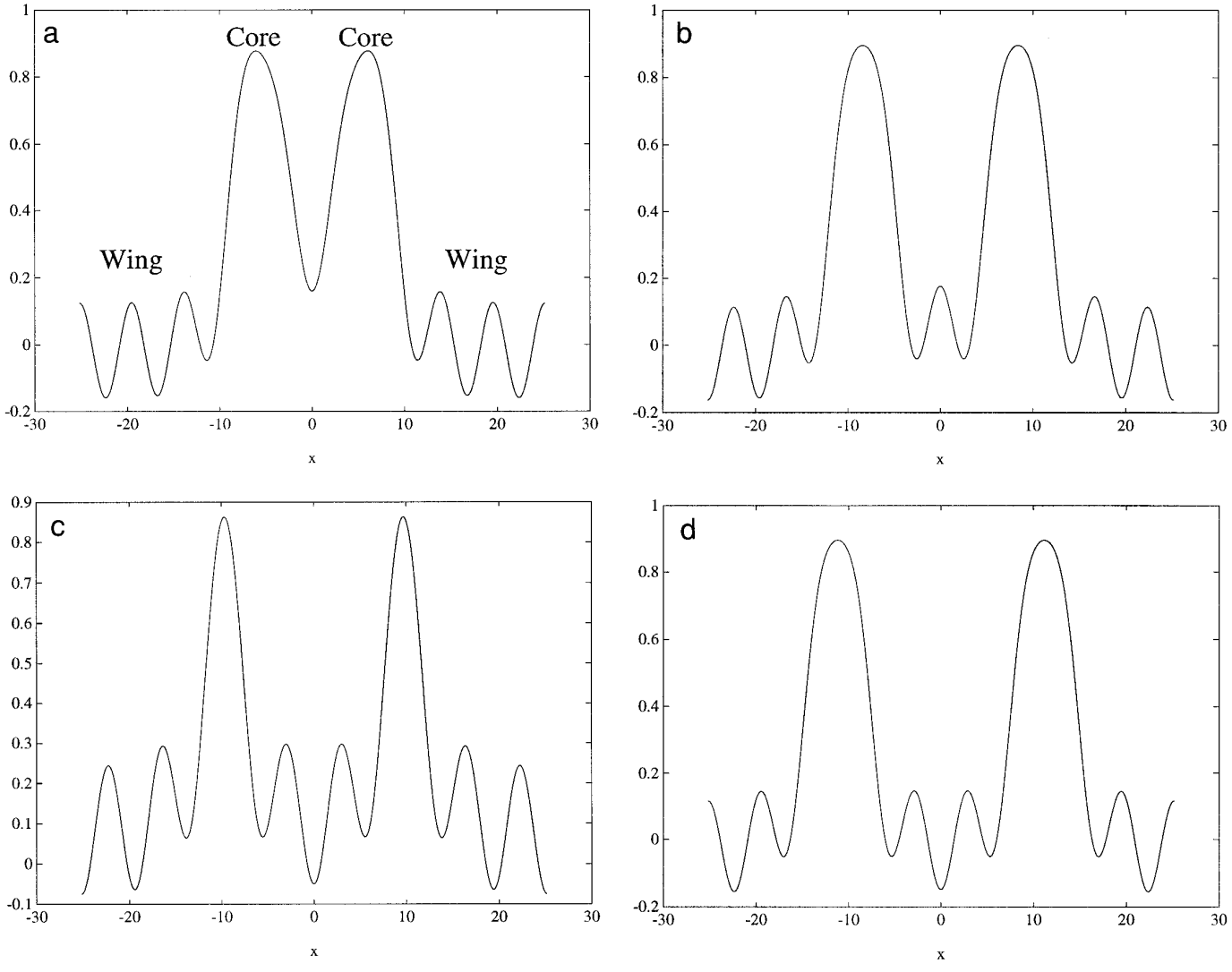

FIG. 1. FKdV nonlocal bions for $\varepsilon = \frac{1}{4}$, which is equivalent to a phase speed $c = 0.3125$. The four modes with the smallest separation between the two big peaks are shown. The maxima are at $x = \pm s$, where (a) $s = 6.07$, (b) $s = 8.41$, (c) $s = 9.69$, and (d) $s = 11.17$.

and extend indefinitely both to the left and the right on the infinite spatial interval.

The FKdV equation also has steadily translating nonlinear solutions on the periodic interval which we shall call "bicnoidal waves." For them, the patterns shown in Fig. 1 are simply repeated on each spatial period. When the period is large in comparison to the width of the cores, the periodic solutions are extremely good approximations to the infinite interval solution (except near the edges of the spatial period).

2. PERTURBATION THEORY FOR TWO WEAKLY OVERLAPPING SOLITARY WAVES

Gorshkov, Ostrovskii, and Papko (GOP) [2, 10–13] and others [3–5] have developed a theory for soliton–soliton interactions. The solitons' *self-interaction* is strong and unapproximated. However, if the solitary waves remain *well separated* during a collision or in a bound state, the *overlap* between the two solitary waves will be small. Since the solitons decay exponentially fast with distance from their maxima, the overlap is exponentially small in the separation S between the two solitary waves. The GOP theory is very general and predicts collision-induced phase shifts and other time-dependent features. However, we shall only discuss the simpler case in which the peaks of the two solitary waves are fixed at $X = \pm s$, where $S \equiv 2s$ is the total peak-to-peak separation of the two solitons.

The first step is to assume that the bion is steadily translating at a phase speed c. In a reference frame travelling with the wave, the partial differential equation (1) becomes the ordinary differential equation

$$u_{XXXXX} + u_{XXX} + (u - c)u_X = 0, \tag{2.1}$$

where

$$X \equiv x - ct. \tag{2.2}$$

The next step is to assume that the exact solution is the superposition of an approximate solution $U(X)$ and a correction $\Delta(X)$, where Δ is assumed to be small:

$$u = U(X) + \Delta(X). \tag{2.3}$$

Substituting this decomposition into (2.1) and neglecting terms of $O(\Delta^2)$ gives the "Newton–Kantorovich" equation for (2.1),

$$J\Delta = -R \tag{2.4}$$

which is the linearization of the original problem with respect to $U(X)$, where J is the linear operator

$$J \equiv \frac{\partial^5}{\partial X^5} + \frac{\partial^3}{\partial X^3} + \{U(X) - c\}\frac{\partial}{\partial X} + U_X \tag{2.5}$$

and $R(U)$ is the "residual function"

$$R(U) \equiv U_{XXXXX} + U_{XXX} + (U(X) - c)U_X \tag{2.6}$$

which is obtained by substituting $U(X)$ into the original differential equation (2.1); $R(U) = 0$ if U is an exact solution.

By repeatedly solving the Newton–Kantorovich equation and updating $U(X)$ via $U \Rightarrow U + \Delta$ at each iteration, we obtain the differential equation version of Newton's iteration. When the differential equation is discretized, J becomes the Jacobian matrix **J** of the discretization of (2.1), and (2.4) becomes the usual Newton (also called "Newton–Ralphson") iteration for solving a system of nonlinear algebraic equations. We computed the numerical solutions throughout the paper by the Newton–Ralphson iteration after applying a pseudospectral Fourier discretization.

The analytic perturbation theory of Grimshaw and Malomed and of Gorshkov, Ostrovskii, and Papko also employs the Newton–Kantorovich equation. In the perturbation theory, $U(X)$ is defined to be the superposition of two exact single soliton solutions,

$$U(X) \equiv U_1(X) + U_2(X), \tag{2.7}$$

where $U_1(X)$ is the soliton whose peak is at $X = -s$ and $U_2(X)$ is that with its maximum at $X = s$. $R(U)$ is then the "overlap" residual

$$R_{\text{overlap}} \equiv U_1U_{2,X} + U_2U_{1,X} \tag{2.8}$$

which has been simplified by exploiting the fact that U_1 and U_2 are *individual* solutions to (2.1).

The quantization condition—bions exist only for *discrete* values of the separation parameter s—arises because the Newton–Kantorovich equation is *insoluble* for *arbitrary* s. The reason is that the solutions to (2.1) are *translationally invariant;* that is, if $u(X)$ is a solution to (2.1), then so also is

$$v(X) \equiv u(X + p), \tag{2.9}$$

where p is an arbitrary constant. This in turn implies that the function

$$e_A(X) \equiv u_X \tag{2.10}$$

must be a *homogeneous* solution of the Newton–Kantorovich equation, that is, an eigenfunction of the Jacobian operator with an eigenvalue of zero. The proof is to Taylor expand (2.9) for $p \ll 1$, substitute into (2.4), simplify using the fact that $R(u) = 0$, and then take the limit $p \Rightarrow 0$. One finds that $u(X + p)$ solves (2.1) in the limit of infinitesimal translation p if and only if $Ju_X = 0$.

The existence of a homogeneous solution to the Newton–Kantorovich equation creates the Fredholm alternative: Either R_{overlap} satisfies a constraint so that it does not project onto the eigenfunction, or the linearized differential equation has no bounded solution. This condition restricts the soliton-to-soliton separation $2s$ to discrete values.

There are two subtleties. The first is that if we integrated (2.1) with respect to X to obtain the equivalent fourth-order form solved in [15], then the Jacobian operator would be self-adjoint and the constraint would be the obvious condition that $R(U)$ must be orthogonal to the homogeneous solution u_X. However, the linearization of the fifth-order equation (2.1) is *not* self-adjoint, and the constraint is orthogonality with respect to the homogeneous solution of the *adjoint* operator J^*.

Define the inner product $\langle a, b\rangle$ to be the integral of the product of $a(X)$ with $b(X)$ for any two functions a, b, where the integral is from $-\infty$ to ∞ for bions and over the spatial period when analyzing bicnoidal waves. The adjoint is then defined by the condition that $\langle a, Jb\rangle = \langle J^* a, b\rangle$ for arbitrary functions a, b. By integrating by parts and comparing the result to (2.1), one can show that $u(X)$ itself is the eigenfunction of J^*; that is,

$$J^*u = 0. \tag{2.11}$$

The constraint then takes the form

$$\langle u, R_{\text{overlap}}\rangle = 0. \tag{2.12}$$

The second subtlety is that Grimshaw–Malomed theory does not actually linearize the FKdV equation with respect to an exact solution $u(X)$, but rather with respect to the superposition of two solitons, $U(X)$. However, it is consistent with the neglect of terms of $O(\Delta^2)$ to approximate $U(X)$ in J by U_1 alone near $X = -s$ and by U_2 alone near $X = s$. With this approximation, we are linearizing with respect to an exact solution $U_1(X)$ near $X = -s$, and therefore the approximate Jacobian

$$\tilde{\mathbf{J}} \equiv \frac{\partial^5}{\partial X^5} + \frac{\partial^3}{\partial X^3} + \{U_1(X) - c\}\frac{\partial}{\partial X} + U_{1,X} \quad (2.13)$$

has U_1 as an exact eigenfunction of its adjoint. The Fredholm constraint (or nonsecularity condition, as it is often called in perturbation theory) is then

$$\langle U_1, R_{\text{overlap}}\rangle = \int U_1(X)\{U_1(X)U_2(X)\}_X\, dX = 0. \quad (2.14)$$

Since the overlap is largest at $X = 0$, one may approximate the solitons in (2.14) by their asymptotic forms as $|X| \Rightarrow \infty$ with an error which is exponentially small in the separation parameter s; if this error is not small, the perturbation is no good anyway.

If the solitons decay monotonically like those of the ordinary Korteweg–deVries equation, which asymptote to $U_1(X) \sim \exp(-2\varepsilon|X + s|)$ for some constant ε, then it is easy to see that the integrand in (2.14) is one-signed and can never vanish. Thus, bound states of solitons are not possible for the KdV equation or for any species of solitons which decay monotonically for large $|X|$.

The weakly nonlocal solitons of the FKdV equation (2.1) do in fact decay monotonically, but not to zero, but rather to the oscillation

$$U_1(X) \sim \alpha(\varepsilon)\,\sin(k_f(\varepsilon)[X + s] + \Phi), \quad |X + s| \gg 1, \quad (2.15)$$

where ε, the pseudowavenumber, is a parameter related to the phase speed c by the exact solution $c = 4\varepsilon^2 + 16\varepsilon^4$. It is the overlap of these oscillatory wings that permits the constraint (2.14) to be satisfied—but only for *discrete* values of the separation parameter s.

The oscillations of the solitons in the "far field" where $|X| \gg 1$ also creates some additional formal difficulties which are raised, but not completely resolved, in Grimshaw and Malomed [1]. Nevertheless, we shall show that the prediction of bions, that is, solitary waves with two large maxima instead of just one, are confirmed by our numerical results, as is the quantization condition.

Grimshaw and Malomed further predict that, since the amplitude of the oscillations α is an *exponentially decreasing* function of $1/\varepsilon$, whereas the amplitude of the cores is a function only of ε^2, there is a minimum peak-to-peak separation for a given ε (or equivalently, a given phase speed c or core amplitude) which rapidly increases as ε decreases. To put it another way, it is only when the solitons are sufficiently far apart to have decayed to the oscillations displayed in (2.15) at $X = 0$ that these oscillations can make the orthogonality constraint be obeyed. This prediction of a rapidly increasing minimum s is verified, too.

Nevertheless, many interesting questions remain. In the next four sections, we ask: How are these eigenfunctions of J and its adjoint reflected in the numerical analysis?

3. NEARLY SINGULAR EIGENMODES IN NEWTON'S ITERATION

The heart of the Grimshaw–Malomed theory is that the Jacobian operator is singular. This would seem to imply that a numerical computation of bions via Newton's iteration would explode in overflow errors and stern warnings: Matrix is singular!

In reality, the numerical difficulties are not that bad—and yet the translational eigenfunction does play a crucial and dominant role in Newton's method. The first saving grace is that, although a rigorous argument is still lacking, a couple of pieces of evidence suggest that FKdV solitons and bions must be *symmetric* about some point which we will choose, without loss of generality, to be $X = 0$.

Symmetry with respect to $X = 0$ means that $u(X) = u(-X)$ for all X. Grimshaw and Joshi [14] have proved that nonlocal, steadily translating structures must be symmetric for *large* $|X|$. However, their argument does not exclude the possibility of an unsymmetric core. Boyd [15] tried to numerically compute asymmetric solitary waves, but failed even when the spectral basis was constrained to be unsymmetric. We exploit this symmetry by employing a spectral basis which uses only symmetric functions—a cosine series to compute bicnoidal waves, for example.

The exact translational eigenfunction, $e_A(X) \equiv u_X$, is *antisymmetric,* however, because differentiation is a parity-reversing operation. (This is obvious if one recalls that the derivative of a Fourier cosine series is a sine series.) Therefore, a symmetric basis automatically excludes the homogeneous solution of the Newton–Kantorovich equation; therefore the Jacobian matrix, which is just the discretization of the operator J in (2.4), is nonsingular. Hurrah! In fact, the translational eigenfunction is not even a minor problem for computing ordinary solitary waves.

Unfortunately, the Jacobian matrix for computing bions and bicnoidal waves is *almost* singular. One can show that the function

$$\tilde{e}_S(X) \equiv U_{1,X} - U_{2,X} \quad (3.1)$$

is an *approximate, symmetric* eigenfunction of the Jacobian

by the following arguments. First, it is easy to prove that this is symmetric with respect to $X = 0$ by replacing X by $-X$ and applying the antisymmetry of $U_{1,X}$ and $U_{2,X}$ with respect to the center of solitons one and two, respectively. Second, note that in the vicinity of soliton one, we can neglect $U_{2,X}$ in (3.1) and the terms in U_2 in the Jacobian operator because these will be exponentially small if the two peaks are well separated. With these approximations, however, $\tilde{J}\,\tilde{e}_S \approx 0 + O(\exp(-4\varepsilon\, s))$, where the error term is the magnitude of the second soliton in the vicinity of the first. Thus, besides an *exact* eigenfunction which is antisymmetric with respect to $X = 0$, the Jacobian operator also has an *approximate* eigenfunction which is symmetric and closely resembles $\tilde{e}_S(X)$.

Figure 2 illustrates the eigenfunction of smallest eigenvalue for the Jacobian matrix which is the pseudospectral discretization of the FKdV equation (2.1) using a basis of Fourier cosines. Also shown is the corresponding eigenfunction of $\mathbf{J}^{\mathrm{T}}$, the transpose of the Jacobian, which is the discretization of the adjoint operator J^*. (The pseudospectral method is explained in the Appendix.) Exactly as predicted from the work of Grimshaw and Malomed, the eigenfunction of $\mathbf{J}$ closely resembles u_X as made even clearer in Fig. 2b while the eigenfunction of J^* has the structure of $u(X)$ itself.

Table I shows the corresponding eigenvalues. The second eigenvalue is less than double that of the first; graphs show that it (and the eigenfunction of the transpose) are very similar to those for the lowest mode. For larger ε, these two modes merge to form a complex conjugate pair with complex eigenvalues! Nevertheless, as we shall see from the iteration history illustrated in the next section (where ε is large enough so that the lowest Jacobian eigenvalues are complex), the later iterations are still dominated by corrections that closely resemble u_X.

We can escape the murky confusion of complex eigenvalues by using the singular value decomposition (SVD) of the Jacobian matrix instead. The solution to the matrix equation $\mathbf{Jd} = -\mathbf{R}$, where $\mathbf{d}$ is the column vector of the coefficients of $\Delta(X)$, can be written as

$$\mathbf{d} = -\mathbf{V}\mathbf{W}^{-1}\mathbf{U}^{\mathrm{T}}\mathbf{R}, \tag{3.2}$$

where $\mathbf{V}$ and $\mathbf{U}$ are orthogonal square matrices and $\mathbf{W}$ is a diagonal matrix whose elements are the "singular values" of $\mathbf{J}$, that is, the eigenvalues of $\mathbf{JJ}^{\mathrm{T}}$. The singular values and the columns of $\mathbf{V}$ and $\mathbf{U}$ are always real-valued even when the matrix $\mathbf{J} = \mathbf{UWV}^{\mathrm{T}}$ has complex eigenvalues.

We see from the second half of Table I that one of the modes of the SVD has a singular value more than a thousand times smaller than those of the other modes. Because the *inverse* of $\mathbf{W}$ appears in (3.2), it follows that modes with tiny singular values will be strongly *amplified* in the solution of the linear equation. The amplitude of the response is controlled by the projection of the residual vector $\mathbf{R}$ onto that column of $\mathbf{U}$ (or row of $\mathbf{U}^{\mathrm{T}}$) associated with the singular mode. If we order the modes so that the smallest singular value is associated with Nth columns of $\mathbf{V}$ and $\mathbf{U}$, then the numerical analogue of the Grimshaw–Malomed constraint is that $(\mathbf{U}^{\mathrm{T}})_N \cdot \mathbf{R} = 0$, where the dot denotes the usual inner product of two vectors and the first vector is the Nth row of the transpose of $\mathbf{U}$. The shape and structure of $\mathbf{U}$ are absorbed into the inner product, so the shape of the amplified *response* is that of $\mathbf{V}_N$, the Nth column of $\mathbf{V}$.

Figure 3 illustrates the Nth columns of $\mathbf{U}$ and $\mathbf{V}$. It is not in the least surprising that the resonant column of $\mathbf{U}$ strongly resembles $\mathbf{u}(X)$ while the resonant column of $\mathbf{V}$ resembles U_X, which are also shown for comparison. (More precisely, $\mathbf{V}_N$ resembles the approximation $\tilde{e}_S(X)$ defined by (3.1).) The main difference, evident also in the graphs of the Jacobian eigenmode in Fig. 2, is that $\mathbf{V}_N$ lacks the far field oscillations which are evident in u_X. We offer no explanation for this.

4. ITERATION HISTORY

Figure 4 illustrates the first four corrections $\Delta(X)$ as computed by the Newton–Kantorovich iteration. All later corrections closely resemble $\Delta^{(4)}$. These in turn resemble u_X and therefore the translational eigenfunction of the Jacobian operator and the Nth column of the V matrix in the SVD factorization of the Jacobian matrix. For this reason, u_X is also graphed for comparison.

The main difference between the derivative of the bion and the late corrections is that the former has noticeable oscillations for large $|X - s|$, whereas the oscillations in $\Delta(X)$ rapidly diminish to almost nothing with the iteration number. An oscillation-free (or nearly free) far field is characteristic of the SVD mode, too; there is little doubt that the later iterations are dominated by the nearly singular mode of the Jacobian.

It follows that in later iterations, Newton's method is mostly *translating* the peaks of the solitary waves (so as to change the separation $2s$) *without altering* their *shapes.* (Recall that the singular eigenmode of the Jacobian arises from the *translational* invariance of the FKdV equation.) Because the nearly singular eigenmode or SVD mode is symmetric in X, the two cores move in towards the origin or away from $X = 0$ simultaneously.

For the first iteration or two, however, the quasi-translational mode does *not* dominate. If the first guess is the KdV soliton or the higher order ε power series given below, the first iteration must dress the monotonically decaying core with far field oscillations as evident in Fig. 4a. Only in the "end game," where the solution is very close to its final, converged result does the quasi-translational eigenmode dominate the corrections.

Furthermore, the existence of the nearly singular mode

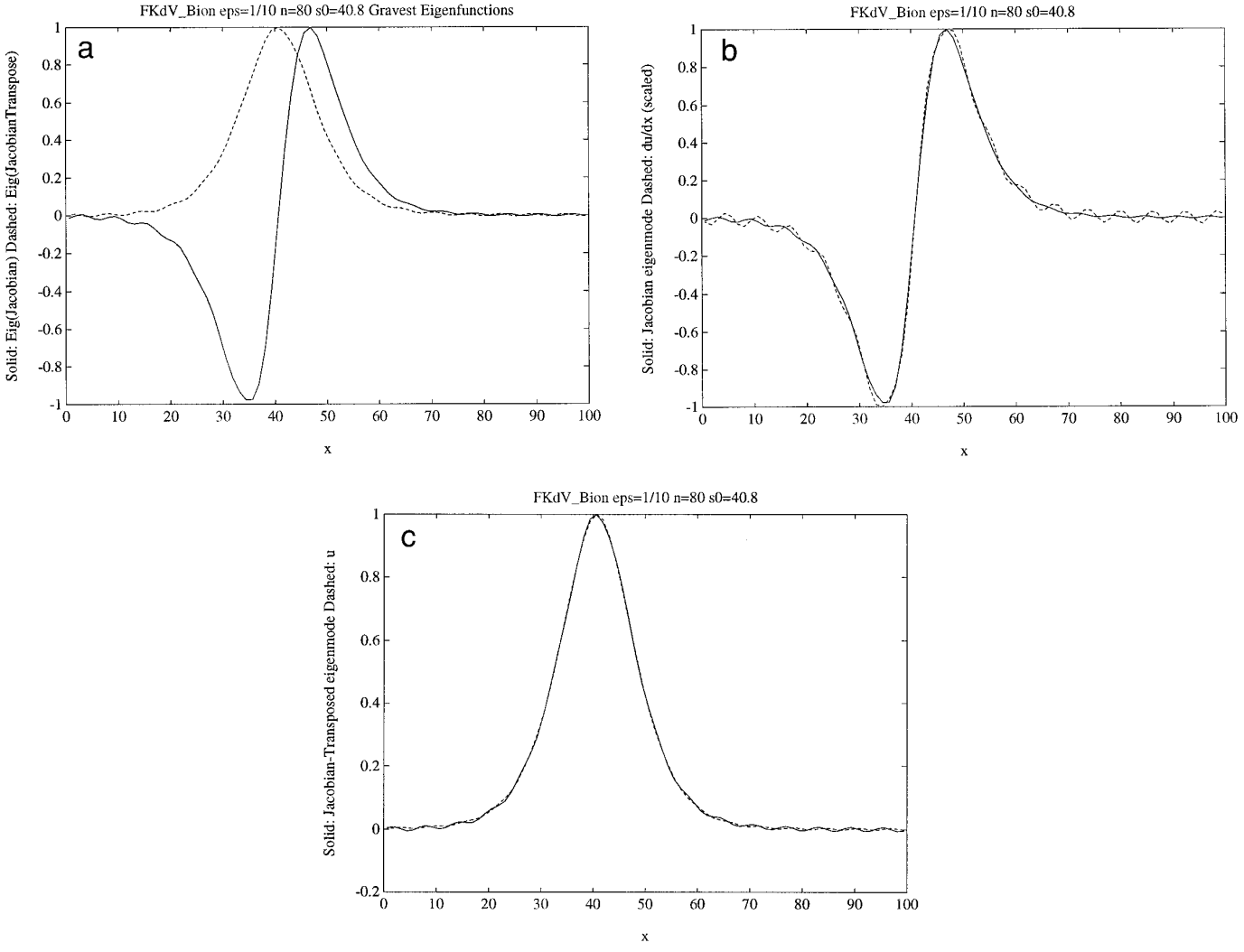

FIG. 2. The gravest eigenfunctions of the Jacobian matrix **J** (pseudospectral representation of the operator J in the Newton–Kantorovich equation) and its transpose for 80 collocation points, $\varepsilon = \frac{1}{10}$ and a spatial period of 200. The Jacobian is computed *after* the iteration has converged to the bion, $u(X)$. Because the eigenfunctions are symmetric with respect to $X = 0$, only the right half of the periodicity interval is illustrated. (a) Solid: gravest eigenfunction of the Jacobian matrix. Dashed: corresponding eigenfunction of the transpose of the Jacobian matrix. (The latter is also said to be a "left eigenfunction" of the Jacobian.) (b) A comparison of the eigenfunction of the Jacobian (solid) with u_X (dashed). (c) A comparison of the eigenfunction of $\mathbf{J}^{\mathrm{T}}$ (solid) with $u(X)$ (dashed).

does not necessarily imply that the Newton iteration will fail or even converge slowly. Although the first guess for Fig. 4 was a KdV soliton with $s_0 = 21$ (versus $s = 21.54$ for the converged solution), the maximum pointwise residual for the first six iterations was (0.053, 0.0021, 0.0012, 1.1×10^{-5}, 2.5×10^{-9}, and 5.3×10^{-14}), where the last is limited by roundoff error.

Figure 5 illustrates the L_∞ norm of the corrections as a function of the initial location s_0 of the soliton on the right half of the interval. The three downward spikes on the dot-dash curve, which connects the maximum pointwise values of the 7th iterate, $\Delta^{(7)}$, point towards the values of s for three solutions which have peaks at 21.54, 22.38, and 24.2. What is remarkable is that after 15 iterations, all computations for which $s_0 > 19.5$ have reduced the residuals at the collocation points to machine roundoff level, $O(10^{-15})$.

Of course, there is a little white lie in this. The graph was computed using discrete steps in s_0, as indicated by the circles on the bottom curve. Because there are multiple solutions, there must be certain values of s_0 for which the iteration is equally attracted to two different solutions and so converges to neither. Figure 5 shows, however, that these intermodal zones of nonconvergence are very small. The nearly singular mode of the Jacobian matrix and the tiny singular value of the SVD factorization of the Jacobian

TABLE I

Eigenvalues and Singular Values of the Jacobian Matrix for 80 Collocation Points, a Period of 200, and $\varepsilon = \frac{1}{10}$

Mode no.	Eigenvalue	Ratio
1	1.42	—
2	−2.68	1.9
3	74.4	52.4
4	−158.1	111.3
Mode no.	**Singular value**	**Ratio**
1	0.0098	—
2	10.3	1051.
3	17.2	1755.
4	30.0	3061

Note. The ratios of these for the higher modes are compared to that for the gravest mode.

matrix do not make the underrelaxed Newton's iteration erratic or unreliable. Rather, the singular quasi-translational eigenmode is important only because it quantizes the solutions that the Newton iteration will converge to.

The singular mode is also important because it determines a minimum allowed value of s for a given ε; for $\varepsilon = \frac{1}{8}$, for example, there are no solutions with the soliton cores closer to the origin than 21.54. A first guess with the soliton peaks at ± 19.5 or smaller will go nowhere fast as indicated by the few circles in the upper left of Fig. 5.

This raises an immediate question: Is it possible to somehow fix up or modify Newton's method? The short answer is: Underrelaxation helps, but there is a complex-valued solution which attracts most bad first guesses, i.e., those that start with the peaks too close together. To understand when underrelaxation succeeds or fails, we must first digress to describe complex-valued solutions, which play a crucial role in the iteration.

5. COMPLEX-VALUED BIONS

The FKdV equation also has complex-valued solutions. One is shown in Fig. 6, which has peaks at ± 19.11.

To compute complex bions, it sufficed to multiply the usual Newton's correction by the factor $(1 + i\Gamma)$, where we chose $\Gamma = \frac{1}{200}$. From $s_0 = 19$, Newton's method generated Fig. 6 in only 10 iterations. There are other complex-valued solutions for a given ε; for example, for $\varepsilon = \frac{1}{8}$, there is a bion rather similar to Fig. 6, except that the peaks are at $X = \pm 16.26$ and the imaginary part is roughly twice as large. (One also needs to use a larger value of Γ to compute it.)

However, the complex-valued bion of the widest core-to-core separation for a given ε has a special significance and will be dubbed the "principal complex bion." This mode is important for two reasons. First, this mode has a special role in attracting—and wrecking—Newton's iteration when the first guess is the sum of two solitary waves which are too narrowly separated for a given ε, as explained in the next section.

Second, the principal complex mode has the smallest

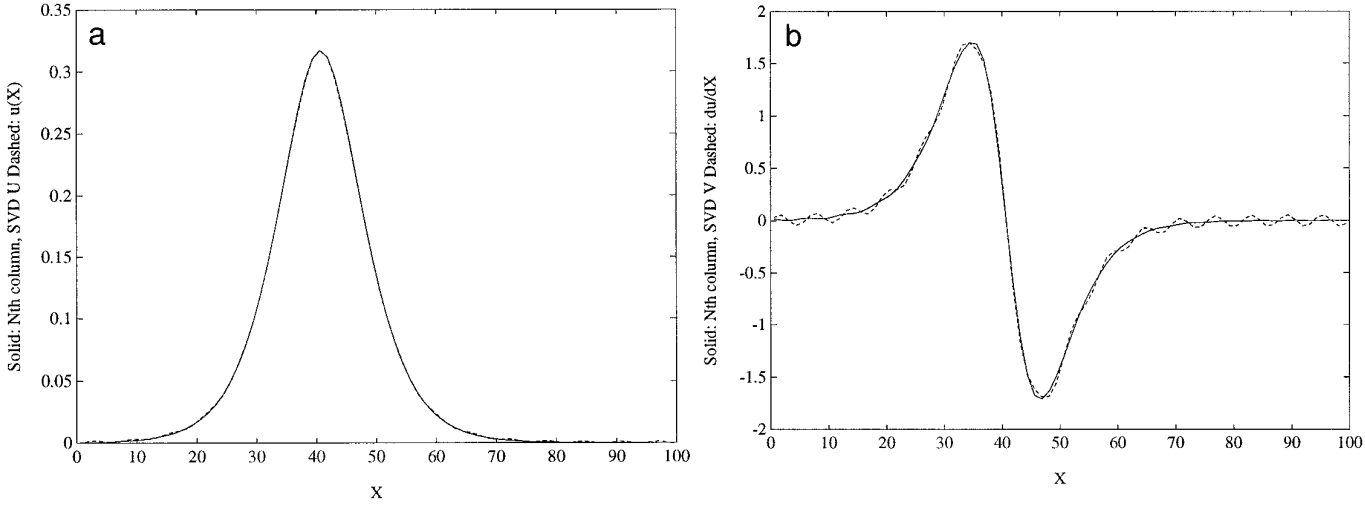

FIG. 3. Structure of SVD modes for the same case as in Fig. 2: 80 collocation points, spatial period of 200, and $\varepsilon = \frac{1}{10}$. (a) Comparison of the Nth column of the $\mathbf{U}$ matrix (solid) with $u(X)$ (dashed). The maximum pointwise difference is only 0.0019. The near-resonant mode will be strongly excited unless the residual vector is orthogonal to $(\mathbf{U}_N)^{\mathrm{T}}$. (b) Comparison of $\mathbf{V}_N$ (solid) with u_X (dashed). The maximum difference is 0.07 and is due almost entirely to that of far field oscillations in the SVD mode. When the Newton's correction Δ is dominated by the (nearly) singular mode of the Jacobian, it will have the shape of $\mathbf{V}_N$.

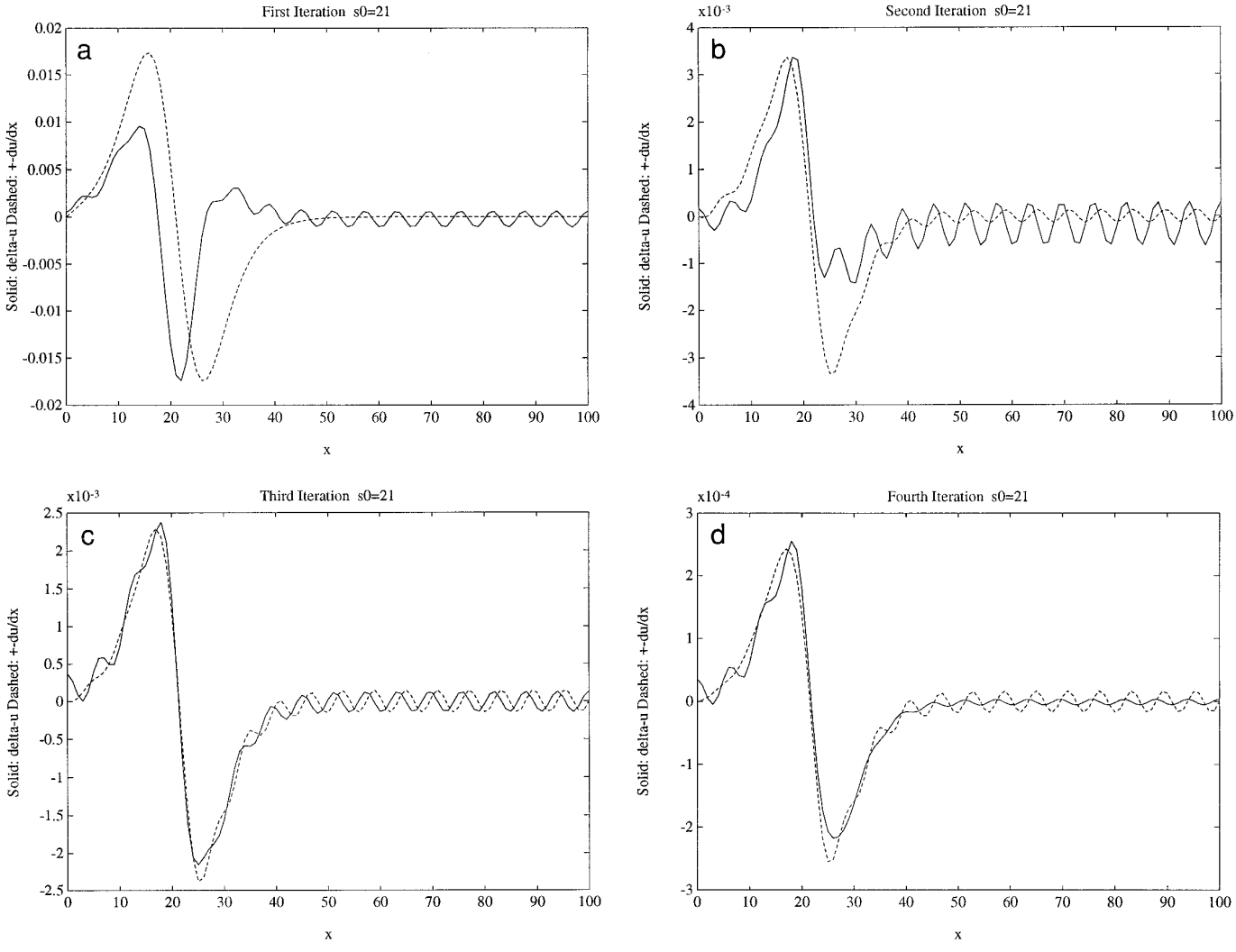

FIG. 4. The first four Newton–Kantorovich iterations for the numerical solution of the FKdV equation for $\varepsilon = \frac{1}{8}$, 60 collocation points and a first guess of $u_0(X) = 12\varepsilon^2 \{\text{sech}^2(\varepsilon[X - 21]) + \text{sech}^2(\varepsilon[X + 21])\}$. Solid: the correction $\Delta(X)$. Dashed: $\pm u_X$/const, where the sign and scaling constant are chosen to produce the closest possible agreement with the correction $\Delta(X)$.

imaginary part of the complex-valued solutions. This has two implications. One is that the real part of this mode is *almost* a steadily translating solution of the FKdV equation. One would expect that if this were used as an initial condition for the time-dependent equation (1.1), this solution would evolve with time rather slowly except for steady propagation.

Third, this almost-bion turns into a true, real-valued bion for larger ε. Figure 7 shows the ratio of the maximum of the absolute value of the imaginary part of $u(X)$ to the real part for a range of ε. At $\varepsilon \approx 0.1299$, the continuation of the complex-valued mode in Fig. 6 merges with its complex conjugate to generate a pair of real-valued solutions.

Figure 8 compares one of these real-valued continuations with the real part of the complex mode of Fig. 6. The bion at larger ε is about 9.5% taller than the real part of the complex solution, but this is almost exactly the 9.8% increase predicted from the approximation of each peak by lowest order perturbation theory, which is proportional to ε^2.

In Section 8, we shall examine the structure of turning points and multiple (real) bions in more detail.

6. UNDERRELAXATION AND THE PRINCIPAL COMPLEX MODE

Both theory and empirical experience show that the domain of convergence of Newton's method can be greatly expanded by underrelaxation; that is, the correction is set equal to the Newton correction multiplied by a constant $\delta \leq 1$:

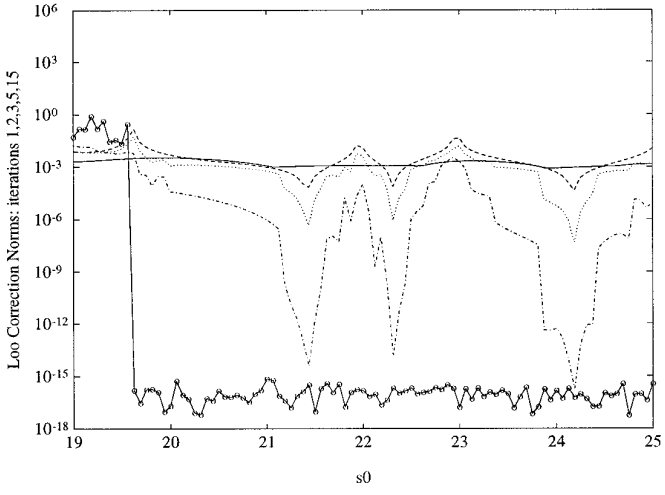

FIG. 5. The L_∞ norm of the corrections Δ for various first guesses and iteration numbers. The first guess $u_0(X)$ was two solitary waves with peaks at $X = \pm s_0$ where s_0 is the horizontal axis of the graphs and the solitary waves were approximated in u_0 by third-order perturbation theory, that is, by terms up to and including $O(\varepsilon^8)$): Solid, first correction; dashed, second iteration; dotted, third Newton correction; dash-dot, fifth iteration; solid-with-circles, 15th iteration. The computations, which specified s_0 at evenly spaced intervals with a spacing of $\frac{1}{16}$, converged (if they converged!) to one of three bicnoidal waves with the peaks at $s = \pm 21.54$, 22.38, and 24.20, respectively. The calculations used 60 collocation points with a spatial period of 200 and $\varepsilon = \frac{1}{8}$.

$$\Delta^{(i)}(X) = \delta_i \Delta^{(i)}_{\text{Newton}}. \tag{6.1}$$

A line search is the usual strategy to determine δ. That is to say, δ_i is chosen to minimize the norm of the residual. We employed a simple inverse powers-of-2 search which evaluated $r(u^{(i)} + \delta_i^{(k)})$ for $\delta_i^{(k)} = (\frac{1}{2})^k$, $k = 1, 2, \ldots, k_{\max}$ and then we chose whichever $\delta_i^{(k)}$ minimized the L_∞ norm of the residual, i.e., the largest absolute value of the biggest element in the vector of the residual at the N collocation points.

In the "end game" close to a root, $\delta_i = 1$, so that this scheme retains the quadratic convergence of the unmodified Newton's algorithm. With a poor first guess, underrelaxation during the "opening game" can often retrieve convergence, where $\delta = 1$ would lead to divergence or a limit cycle.

The theoretical justification for underrelaxation is the

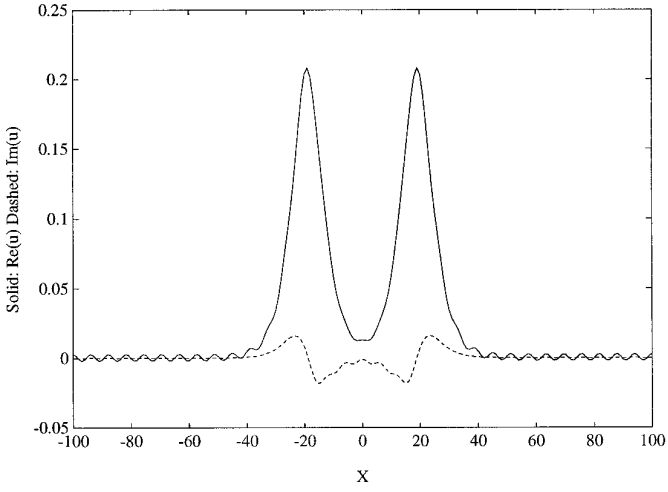

FIG. 6. The real and imaginary parts of the complex-valued solution for $\varepsilon = \frac{1}{8}$ with 80 collocation points, spatial period = 200. The maxima of the real part (solid) are at $X = \pm 19.11$. The maximum value of the real part exceeds that of Im(u) (dashed) by a factor of 11.5.

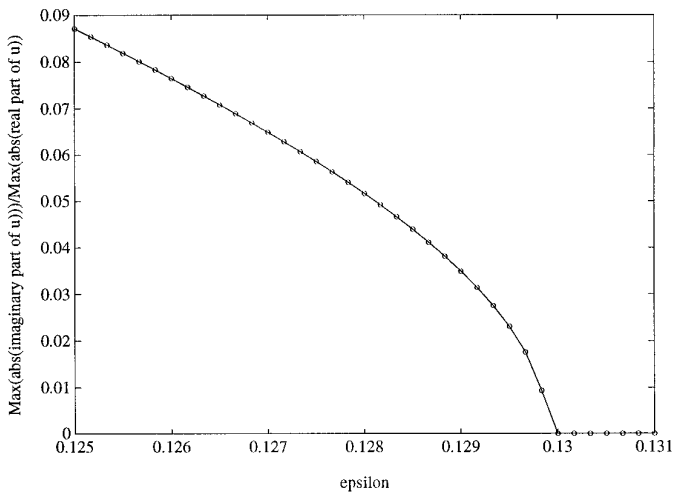

FIG. 7. Ratio of the maximum of the absolute value of the imaginary part of u divided by that for the real part versus ε, same bion branch as Fig. 6.

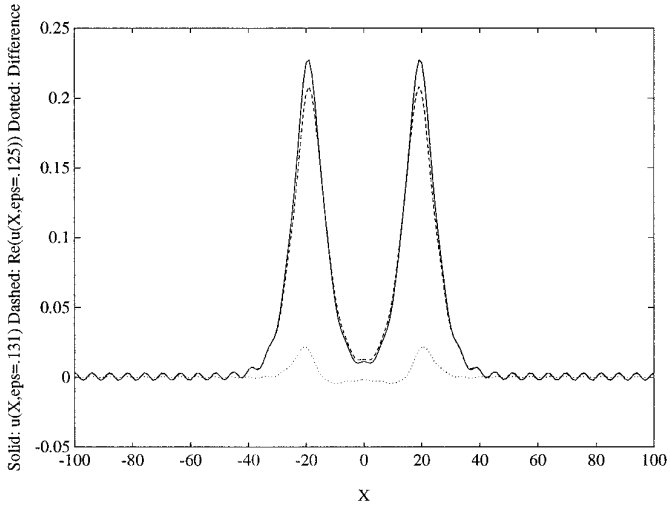

FIG. 8. Solid, $u(X; \varepsilon = 0.131)$; dashed, real part of $u(X, \varepsilon = \frac{1}{8})$; dotted, difference.

concept of the "Newton flow," which is the solution of the system of N ordinary differential equations in the pseudotime variable T,

$$\frac{d\mathbf{u}}{dT} = -\mathbf{J}^{-1}\mathbf{R}, \tag{6.2}$$

where $\mathbf{J}$ is the Jacobian matrix and $\mathbf{R}$ is the column vector of residuals, which are both functions of the column vector $\mathbf{u}$. The standard Newton's iteration, $\mathbf{u}^{(i+1)} = \mathbf{u}^{(i)} - \mathbf{J}^{-1}\mathbf{R}(\mathbf{u}^{(i)})$ is equivalent to solving the Newton flow equation by the Euler forward method with a unit time step. The underrelaxed Newton method is equivalent to applying Euler's scheme with a pseudotime step δ. The crucial point is that the residual is a monotonically decreasing function for the Newton flow; one can prove [17]

$$\mathbf{R}(\mathbf{u}(T)) = \exp(-T)\mathbf{R}(\mathbf{u}(0)). \tag{6.3}$$

This implies that underelaxation will *always* reduce the residual at each step if the pseudotime step δ is sufficiently small.

Unfortunately, the "Newton flow" is singular wherever the Jacobian matrix is singular. In practical terms, this means that even with line search underrelaxation, Newton's iteration can wreck on a reef, where the determinant of the Jacobian is zero. Since $\det(\mathbf{J})$ is a scalar function of N variables, it vanishes on surfaces of dimension $(N-1)$ in the N-dimensional space of unknowns.

Figure 9 is a kind of graphical autopsy of such a shipwreck. The condition number estimate, taken from [16], tends to infinity as $\det(\mathbf{J}) \Rightarrow 0$. Despite the fluctuations, the general trends are clear: The iteration stalls out at a point in the N-dimensional space of unknowns, where $\det(\mathbf{J}) = 0$. The residual norm flattens out, the underrelaxation parameter $\delta \Rightarrow 0$, and the condition number $\Rightarrow \infty$.

When the initial guess for the bion is two peaks separated by a large distance, the underrelaxed iteration is almost always able to find its way home to a real-valued solution. When the initial guess is too narrow—somewhat narrower than any of the real-valued bions for that ε—then usually the iteration fails as in Fig. 9.

In general, the iteration will stall out with $\delta \Rightarrow 0$ near an arbitrary point of the surface where $\det(\mathbf{J}) = 0$. Here, however, the situation is special. As emphasized earlier, the iteration rapidly dresses the solitary waves with far field oscillations so that, except for the first few iterations, the Newton correction is approximately proportional to the translational eigenfunction of the Jacobian matrix. This implies that after the first few iterations for the case in Fig. 9, the shapes of the solitary waves and the far field are correct and the remaining 35 iterations displayed are merely *translating* the soliton peaks to their correct mutual spacing—or trying.

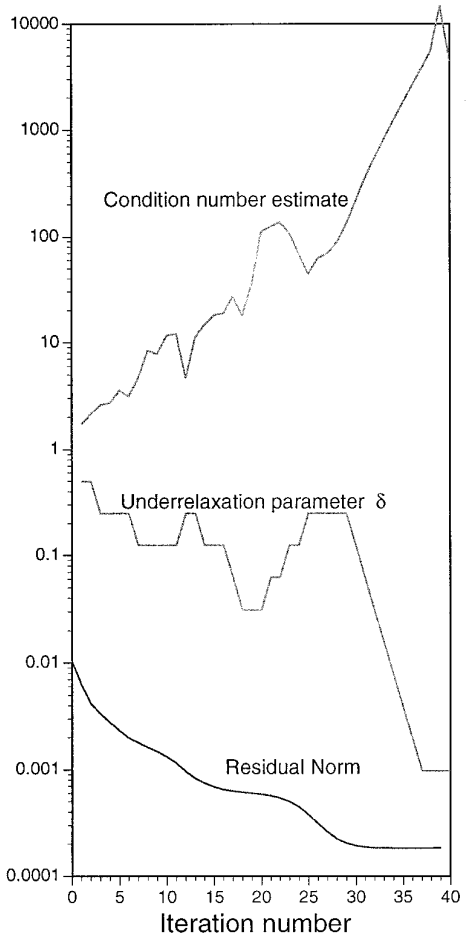

FIG. 9. History of a Newton's iteration that converged to a point where the Jacobian matrix is singular: top, condition number estimate for Jacobian matrix J, divided by 1000; middle, underrelaxation parameter δ; bottom, L_∞ norm of the residual, multiplied by 10. $\varepsilon = \frac{1}{8}$, $s_0 = 8$.

Thus, although the numerical algorithm computes in an N-dimensional space of the Fourier coefficients of $u(X)$, the later iterates represent movement in a one-dimensional subspace only. The iteration will stall out at that peak-to-peak separation, where the residual norm has a local minimum as a function of s, the separation parameter. This happens when s coincides with the separation of the principal complex mode.

Figure 10 shows another typical case. The residual norm decreases slowly, then plunges abruptly when the peaks are at $X = \pm 19.1$—the peaks of the real part of the principal complex bion. The norm of the difference between $u^{(i)}$ and the real part of the complex mode drops steeply at the same time. For larger iteration number i, however, there are only small fluctuations about flat plateaus. The residual can never decrease all the way to zero nor can the difference between the iterates and the real part of the complex solution go to zero because the closest solution is not real,

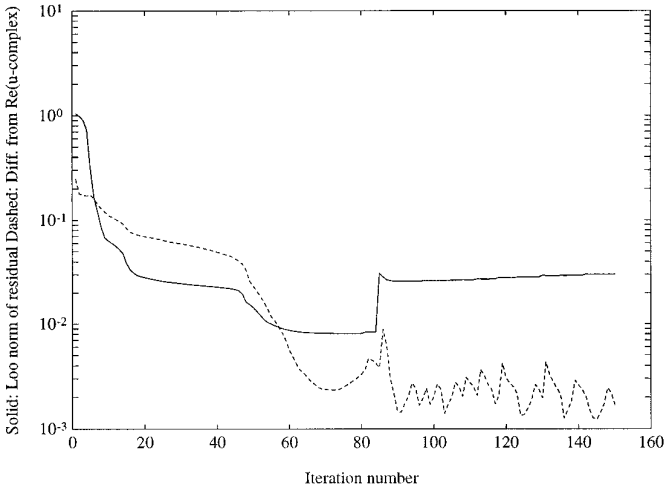

FIG. 10. Solid, L_∞ norm of the residual versus iteration number: Dashed, L_2 norm of the difference between $u^{(i)}(X)$ and the real part of the principal complex mode. The first guess was two solitons as approximated by third order perturbation theory with peaks at ± 5; $N = 40$, $\varepsilon = \frac{1}{8}$.

but complex. (We can reach this complex solution only by allowing the underrelaxation parameter to be complex or making a complex-valued first guess.)

Figure 10 shows that the difference between $u^{(i)}(X)$ and the real part of the complex solution is remarkably small: the maximum difference is only $\frac{1}{100}$ of the maximum of $u^{(i)}(X)$. As it evolves from a narrow first guess (small s_0), the complex mode controls the real-valued iteration, like an arithmetical coral reef, unseen in the hidden waters of the complex-plane, but nonetheless impaling most iterations that are forced to try to cross it.

We must say "most" because occasionally iterations are able to escape from the "reef" and converge to a real-valued bion. This is impossible for the Newton *flow,* but a practical Newton's algorithm moves in *discrete* steps. To permit such escapes, it is sound practice to set a minimum

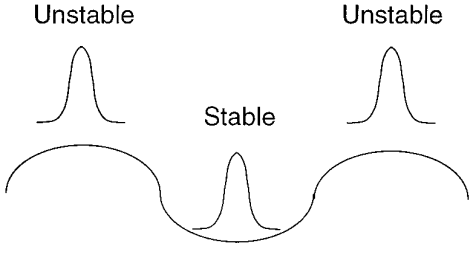

FIG. 11. Schematic of the potential created by the far field of a solitary wave. When another soliton is placed in a valley of the spatially oscillating potential, the result is a *stable* bion. When a soliton is placed on a potential hill, exactly at the maximum, another steadily propagating bion is created. However, this is unstable to small perturbations and the peak-to-peak separation distance will oscillate with time.

TABLE II

Separation Parameter s for Bions ($\varepsilon = \frac{1}{8}$ with a Spatial Period of 200)

	s_m	$s_m - s_m - 1$
*	19.11	Principal complex bion
1	21.54	—
2	22.38	0.84
3	24.20	1.82
4	25.58	1.38
5	27.16	1.58
6	28.65	1.49
7	30.19	1.54
8	31.71	1.52
9	33.24	1.53
10	34.76	1.52
11	36.28	1.52
12	37.81	1.53
13	39.33	1.52
14	40.85	1.52
15	42.38	1.53
16	43.90	1.52
17	45.43	1.53
18	46.95	1.52
19	48.48	1.52
—	50	Ordinary cnoidal wave of period 100

Notes. (1) For these parameters, one-quarter of the far field wavelength is $W_f/4 = 1.524$.

(2) The core-to-core distance is equal to $2s$; the peaks are at $X = \pm s$.

underrelaxation parameter. (We arbitrarily imposed $\delta \geq \frac{1}{1024}$.) With that, or with coarser limits, the iteration sometimes jumps across the reef after several dozen iterates of little change.

Escape occurs because very close to a point, where $\det(J) = 0$, the Newton correction is huge—sometimes large enough to leap into the domain of attraction of a real-valued bion. If so, the line search will accept the jump and then convergence is extremely fast.

Unfortunately, this only happens sometimes, and then usually only after a very large number of iterations. The most effective strategy, as illustrated in Fig. 5, is to try a few iterations for many different initial soliton-to-soliton separations, rather than to use only a few initializations, and to apply hundreds of iterations to each.

7. QUANTIZATION OF PEAK-TO-PEAK SEPARATION

Table II lists the separation parameter s for all the discrete modes that exist for a particular ε and a particular spatial period. Throughout this article, the numerical calculations were performed by choosing a particular value of the phase speed c and then computing the Fourier coefficients as described above and in the Appendix. To label graphs, however, we use ε, which specifies the width of

the KdV solitary wave that best approximates the two cores of the bion via $u_{\rm sol}(X) \sim 12\varepsilon^2\ {\rm sech}^2(\varepsilon X) + O(\varepsilon^4)$. The phase speed is related to ε, *without approximation,* by $c = 4\varepsilon^2 + 16\varepsilon^4$.

Table II confirms the quantization predicted by Grimshaw and Malomed [1]. That is, to say, bions exist only when the distance $2s$ between the two maxima is equal to a set of discrete values.

Since the far field oscillations are essential to binding the two solitons together, the gaps between different allowed values of s should be proportional to the wavelength of those oscillations, which is

$$W_f = \frac{2\pi}{k_f} = \frac{2\pi}{\sqrt{1+4\varepsilon^2}} + O(\alpha^2), \tag{7.1}$$

where k_f is the far field wavenumber and the error is proportional to the square of α, the amplitude of the far field oscillations. Table II shows that for large mode number m,

$$s \sim {\rm const} + mW_f/4 \tag{7.2}$$

which implies that the peak-to-peak distance S $(=2s)$ increases by one-half of the far field wavelength from one bion mode to the next.

Malomed and Grimshaw [1] claim that the bion modes differ by *integer,* rather than half-integer, multiple of W_f. However, this is only a difference in convention. Figure 11 is a schematic that shows that the potential energy created, in the GOP theory, by one solitary wave is oscillatory with X. If a second soliton is placed in a valley, any valley, of the potential energy, it will create a *stable* stationary state (''stationary'' in a frame of reference moving at the common phase speed of the two solitary waves). Placing a soliton on a hill of the potential, exactly at the top, will also make a stationary state. These bions will be *unstable* because small perturbations will trigger large oscillations in core-to-core separation as the soliton rolls down the potential hill.

Since our numerical method solves an ordinary differential equation in the moving reference frame, it happily computes *all* stationary states, both stable and unstable. Malomed and Grimshaw [1] specified only the change in core-to-core distance between different *stable* bions (B. Malomed, private communication.) This is indeed mW_f, where m is an *integer.*

Thus, every other bion listed in Table II is unstable. Identifying which modes are stable could be done by solving the time-dependent FKdV equation using the output of the Newton/pseudospectral algorithm as the initial condition (plus a tiny perturbation).

Figure 12 compares two bions that differ by $W_f/2$ in core-to-core distance (Fig. 12a) and by W_f (Fig. 12b). The small oscillations in the latter graph are out of phase (differ by sign) both between the cores and in the far field. The pair of modes which differ by only half the far field wavelength have small oscillations which are in phase between the two cores, but are of opposite signs for large $|X|$.

However, the table also shows that the spacing is quite irregular for the lowest few modes, i.e., those bion modes that have the smallest separation. The Malomed–Grimshaw theory is clearly successful, but there is room for further refinements.

8. TRACING THE BRANCHES

By using pseudoarclength continuation [18] with the Fourier pseudospectral method [19], we traced the bion modes as ε varied. Figure 13 shows the variation of the lowest Fourier coefficient for the lowest modes. The lower right-hand side of each branch is one of the four solutions illustrated in Fig. 1.

As ε decreases from its initial value of $\frac{1}{4}$, each branch has a turning point; for smaller ε, the branches continue only as the sort of complex-valued bions discussed above. Remarkably, the branches also have turning points at larger ε and then reverse backwards to smaller ε.

Figure 14 is a cartoon depicting the fourth branch bions at both turning points and at the extremes of the graph. The far field oscillations are so large at the extremes that the wave is not ''weakly'' nonlocal in any meaningful sense, so we have not continued the graphs beyond the range illustrated. Still, even on that interval $\varepsilon \in [\frac{1}{10}, \frac{1}{4}]$, the bion displays remarkable diversity while retaining the basic pattern of two large peaks projecting up from a sea of background oscillations.

9. SUMMARY

Our numerical calculations verify the important predictions of the perturbation theory of Grimshaw and Malomed, including the following:

(i) FKdV solitary waves form bound states.

(ii) The distances between the peaks in the bion are quantized, that is, limited to discrete values.

(iii) For a given amplitude, there is a bion of minimum separation. As the amplitude decreases, this minimum separation rapidly increases.

However, we also found new features which are not in the theory. The irregular gaps in separation parameter s for small mode number, the existence of bions with strongly overlapping cores, and the turning points which mark transitions from real-valued bions to complex-valued solutions

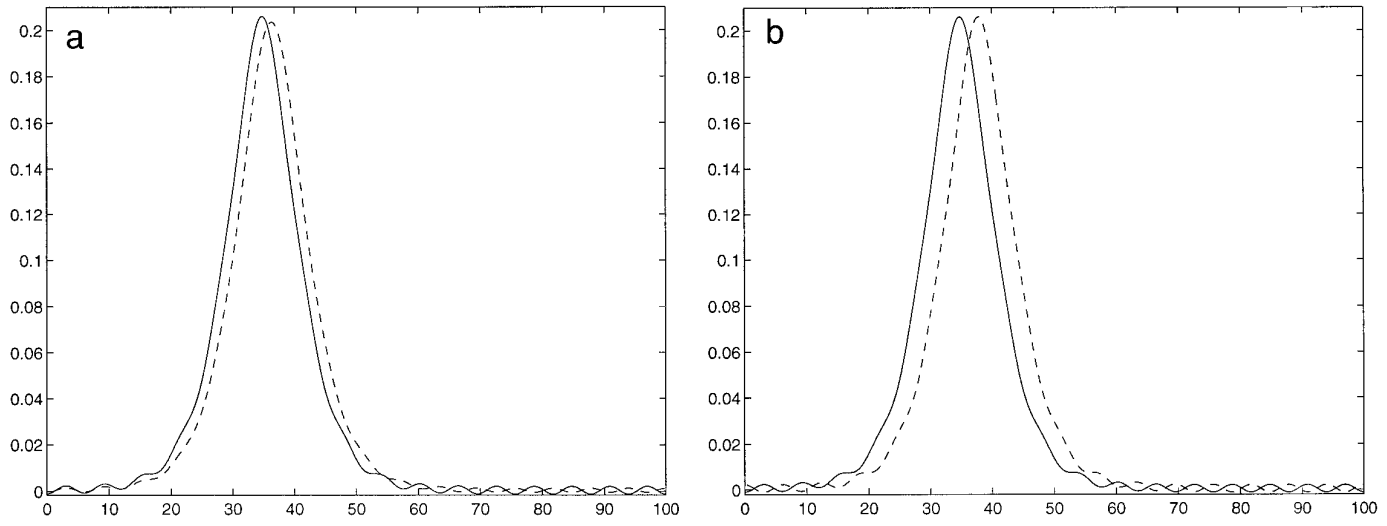

FIG. 12. Comparison of neighboring bion modes: (a) Two adjacent modes for which s differs by the minimum possible, $W_f/4$, where W_f is the wavelength of the far field oscillations ($\varepsilon = \frac{1}{8}$, spatial period = 200): Solid, $s = 34.76$; dashed, $s = 36.28$. (b) Two adjacent modes for which s differs by twice as much as in (a): solid, $s = 34.76$; dashed, $s = 37.81$.

as $\varepsilon \Rightarrow 0$ are experimental discoveries which lay beyond the scope of their analysis.

One unresolved issue is to systematically trace the complicated structure of the various bion branches. We have made a start, but our graphs are representative rather than comprehensive.

Some other intriguing questions remain, too. Why does a given bion mode always become complex at small amplitudes? Why do the real-valued solutions have multiple turning points on each branch? What is the physics behind some of the rather strange-looking coherent structures which appear as the branches are traced? There is much room for future work.

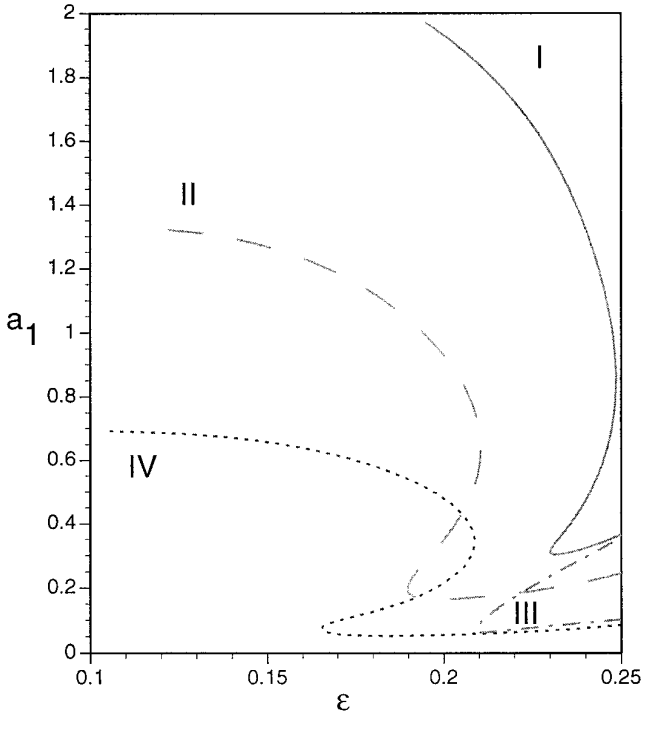

FIG. 13. The lowest Fourier coefficient a_1 versus ε for the four branches of solutions whose forms for $\varepsilon = \frac{1}{4}$ are illustrated in Fig. 1. The spatial period is 16π. The values of the separation parameter at the lower right-hand side of each branch are as follows: (I) $s = 6.07$ (solid); (II) $s = 8.41$ (dashed); (III) $s = 9.69$ (dot-dash); (IV) $s = 11.17$ (dotted).

APPENDIX: THE NEWTON–KANTOROVICH/FOURIER PSEUDOSPECTRAL ALGORITHM

The Newton–Kantorovich iteration for (2.1) begins with a first guess. We usually employed third-order perturbation theory, that is,

$$u^{(0)} = u_{\text{sol}}(X - s) + u_{\text{sol}}(X + s) \tag{A.1}$$

$$\begin{aligned} u_{\text{sol}}(X) \sim\ & 12\varepsilon^2 \operatorname{sech}^2(\varepsilon X) + 120\varepsilon^4\{\tfrac{3}{2}\operatorname{sech}^4(\varepsilon X) - \operatorname{sech}^2(\varepsilon X)\} \\ & + \varepsilon^6\{5580 \operatorname{sech}^4(\varepsilon X)[\operatorname{sech}^2(\varepsilon X) - 1] \\ & + 360 \operatorname{sech}^2(\varepsilon X)\} + \varepsilon^8\{297972 \operatorname{sech}^8(\varepsilon X) \\ & - 397296 \operatorname{sech}^6(\varepsilon X) + 126216 \operatorname{sech}^4(\varepsilon X) \\ & - 14832 \operatorname{sech}^2(\varepsilon X)\}, \end{aligned} \tag{A.2}$$

except for $\varepsilon = \frac{1}{4}$, where we employed only the $O(\varepsilon^2)$ approximation. To iterate, we solve the Newton–Kantorovich differential equation

$$J^{(i)}\Delta^{(i)} = -R(u^{(i-1)}), \tag{A.3}$$

where R is the residual function

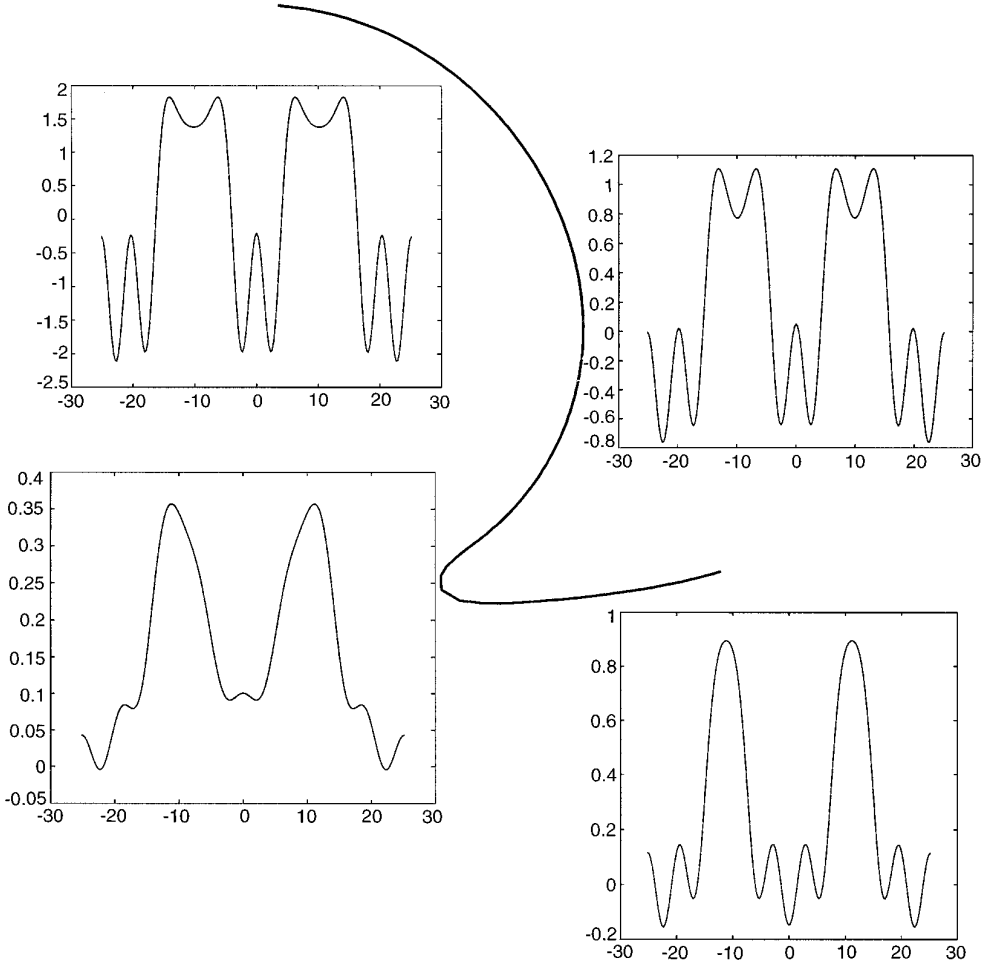

FIG. 14. Solid: $a_1(\varepsilon)$ for Branch IV of the previous Fig. The four inserts show $u(X)$ for four points on the branch. Upper left: $\varepsilon = 0.116573$ (left end of the branch). Bottom left: $\varepsilon = 0.165639$, which is a turning point. Upper right: $\varepsilon = 0.208756$, which is the other turning point. Bottom right: $\varepsilon = 0.25$ (right limit of the branch). The branch continues beyond the range in ε which is illustrated, $\varepsilon \in [0.116, 0.25]$.

$$R(u^{(i)}) \equiv u^{(i)}_{XXXXX} + u^{(i)}_{XXX} + (u^{(i)}(X) - c)u^{(i)}_X \quad \text{(A.4)}$$

and J is the Jacobian operator

$$J^{(i)} \equiv \frac{\partial^5}{\partial X^5} + \frac{\partial^3}{\partial X^3} + \{u^{(i-1)}(X) - c\}\frac{\partial}{\partial X} + u^{(i-1)}_X, \quad \text{(A.5)}$$

and then we perform the update

$$u^{(i)} \equiv u^{(i-1)} + \delta_i \Delta^{(i)} \quad \text{(A.6)}$$

until the norm of $\Delta^{(i)}$ is below some tolerance.

The underrelaxation parameter is chosen by a line search to minimize the norm of $R(u^{(i-1)} + \delta_i\Delta^{(i)})$ for $\delta \in [\delta_{\min}, 1]$. The parameter $\delta_{\min}$ ($=\frac{1}{1024}$ in most of our computations) ensures that there is always some movement from one iteration to the next. Exact minimization is wasteful and unnecessary in current arithmetical folklore, so we merely evaluated the residual for a set of discrete values of δ and then chose whichever one gave the smallest norm. For simplicity, the discrete δ were chosen to be 2^{-k}, where k is a nonnegative integer.

The linearized differential equation (A.3) is discretized by expanding $u(X)$ and $\Delta(x)$ as Fourier cosine series with a prespecified mean:

$$u(X) = u_{\text{mean}} + \sum_{j=1}^{N} a_j \phi_j(X) \quad \text{(A.7)}$$

$$\Delta^{(i)}(X) = \sum_{j=1}^{N} d_j^{(i)} \phi_j(X), \quad \text{(A.8)}$$

where u_{mean} is a constant and where the basis functions are

$$\phi_j(X) = \cos(jX/L), \quad j = 1, ..., N, \tag{A.9}$$

where L is the spatial period P divided by 2π.

The first remark is that we approximate bions, which technically are defined only on $X \in [-\infty, \infty]$, by spatially periodic solutions or bicnoidal waves. There are two reasons for this. One is that bicnoidal waves are legitimate solutions of the FKdV equation and interesting in their own right. The second is that the difference between the bicnoidal wave and the corresponding bion of the same phase speed decreases exponentially fast with the period P, provided we limit the comparison to $X \in [-P/2, P/2]$. This was explicitly demonstrated for solitons in [15], where the wave equation was solved directly on the infinite interval and the solitary wave was compared with the corresponding cnoidal wave. The argument applies to bions without change.

The second surprise in (A.7) is the restriction to cosines. This restriction builds the expected symmetry of the solutions ($u(X) = u(-X)$ for all X) into the basis set. Also, the cosine-only basis excludes the antisymmetric-with-respect-to-X translating eigenmode of the Jacobian operator. (The *nearly* singular *symmetric* eigenmode of J, linearized with respect to the bion, remains, alas, and causes the complications described in the main body of the paper.)

The third surprise is that the constant in the Fourier cosine series is always 0 for the correction and may be specified *a priori* for $u(X)$. The reason is that if $u(X; c_0)$ is a solution to (2.1), then it is easy to prove by direct substitution that $v(X) \equiv g + u(X; c_0)$ is a solution for $c = c_0 + g$, where g is an arbitrary constant. It follows that the sole effect of adding a constant g to the mean value of $u(X)$, u_{mean}, is to shift the phase speed by g. We lose no generality by specifying u_{mean} *a priori.*

Since we want solitons to decay to the far field oscillations as $|X| \Rightarrow 0$, we made the choice

$$u_{\text{mean}} = 48\varepsilon/P \tag{A.10}$$

which is the mean value of the sum of *two* functions each with the shape of $12\varepsilon^2 \operatorname{sech}^2(\varepsilon X)$.

The pseudospectral discretization, also known as "collocation" or "orthogonal collocation," is to demand that the differential equation should be exactly satisfied at each of the N collocation points

$$X_j = \pi jL, \quad j = 0, 1, ..., (N-1) \tag{A.11}$$

The residual function R becomes the residual vector $\mathbf{R}$ with elements

$$R_j^{(i)} \equiv \{u_{XXXXX}^{(i)} + u_{XXX}^{(i)} + (u^{(i)}(X) - c)u_X^{(i)}\}|_{X=X_j} \tag{A.12}$$

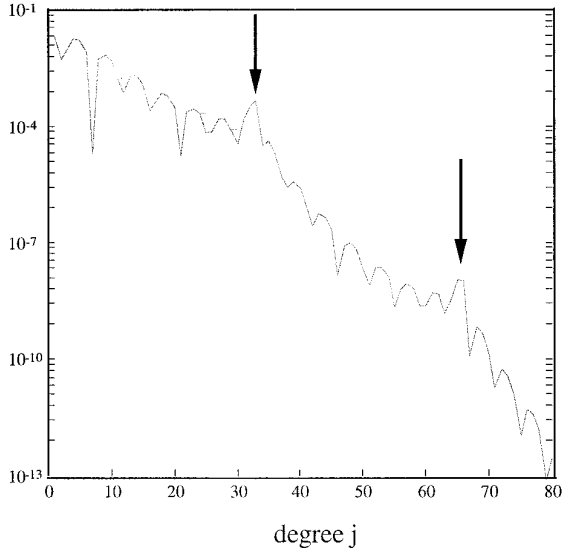

FIG. 15. $|a_j|$ versus j for the first mode bion (bicnoidal wave) with a spatial period of 200, $\varepsilon = \frac{1}{8}$, 80 collocation points, and maxima at $X = \pm 21.54$. The arrows point to the resonance spike at the far field wavenumber, $k_f \approx 1 \Leftrightarrow j = 32$ for this spatial period, and to its second harmonic at $j \approx 64$. Both the far field and the soliton cores are extremely well resolved!

while the Jacobian operator becomes the Jacobian matrix $\mathbf{J}$ with elements

$$\begin{aligned} J_{jk}^{(i)} = {} & \phi_{k,XXXXX}(X_j) + \phi_{k,XXX}(X_j) \\ & + (u^{(i-1)}(X_j) - c)\phi_{k,X}(X_j) \\ & + u_X^{(i-1)}(X_j)\phi_k(X_j). \end{aligned} \tag{A.13}$$

The matrix equation $\mathbf{Jd} = -\mathbf{R}$ is solved for the column vector $\mathbf{d}$ whose elements are the spectral coefficients of $\Delta^{(i)}(X)$.

The spectral coefficients for $u(X)$ exhibit the exponential rate of decay with j which is usual for Fourier coefficients of smooth functions [19] as illustrated in Fig. 15.

One final note: because the Jacobian matrix $\mathbf{J}$ operates on a vector of spectral coefficients, but generates Ju as evaluated at the collocation points, it follows that the eigenvectors of $\mathbf{J}$ are spectral coefficients, where those of $\mathbf{J}^{\mathrm{T}}$ are vectors of grid point values. For graphical display, the eigenvectors of the Jacobian matrix have been converted to grid point values by summing the Fourier series at each of the grid points and then graphically compared with u_X and similarly for the eigenmodes of the SVD factorization.

To follow the modes around branch points, we used pseudoarclength continuation [18, 20].

ACKNOWLEDGMENTS

This work was supported by the NSF through Grants OCE8812300, DMS8716766, and ECS9012263 and by the Department of Energy

through Grant KC070101. I thank Roger Grimshaw and David Broutman for inviting me to visit the Universities of Melbourne and New South Wales, where this article was conceived, and the Australian Research Council for partial support of my trip.

REFERENCES

1. R. H. J. Grimshaw and B. A. Malomed, *J. Phys. A* **26,** 4087 (1993).
2. K. A. Gorshkov and L. A. Ostrovskii, *Physica D* **12,** 424 (1981).
3. V. I. Karpman and V. V. Solov'ev, *Physica D* **12,** 142 (1981).
4. J. P. Boyd, *Physica D* **21,** 227 (1986).
5. B. A. Malomed, *Phys. Rev. A* **44,** 6954 (1991).
6. J. P. Boyd, "New Directions in Solitons and Nonlinear Periodic Waves: Polycnoidal Waves, Imbricated Solitons, Weakly Non-local Solitary Waves and Numerical Boundary Value Algorithms," in *Advances in Applied Mechanics,* Vol. 27, edited by T.-Y. Wu and J. W. Hutchinson (Academic Press, New York, 1989), p. 1.
7. J. P. Boyd, "Weakly Non-local Solitary Waves," in *Nonlinear Topics in Ocean Physics,* edited by A. R. Osborne and L. Bergamasco (North-Holland, Amsterdam, 1991), p. 527.
8. J. P. Boyd, Weakly nonlocal solitary waves and other exponentially small phenomena, to be published.
9. H. Segur, S. Tanveer, and H. Levine (Eds.), *Asymptotics Beyond All Orders* (Plenum, New York, 1991).
10. K. A. Gorshkov, L. A. Ostrovskii, and V. V. Papko, *Sov. Phys. JETP* **44,** 306 (1976).
11. K. A. Gorshkov, L. A. Ostrovskii, and V. V. Papko, *Sov. Phys. Dokl.* **22,** 378 (1977).
12. K. A. Gorshkov and V. V. Papko, *Sov. Phys. JETP* **46,** 92 (1977).
13. K. A. Gorshkov, L. A. Ostrovskii, V. V. Papko, and A. S. Pikovsky, *Phys. Lett. A* **74,** 177 (1979).
14. R. H. J. Grimshaw and N. Joshi, *SIAM J. Appl. Math.* **53,** 124–135 (1995).
15. J. P. Boyd, *Physica D* **48,** 129 (1991).
16. J. E. Dennis Jr., and R. B. Schnabel, *Numerical Methods for Unconstrained Optimization and Nonlinear Equations* (Prentice–Hall, Englewood Cliffs, NJ, 1983).
17. M. T. Chu, On the continuous realization of iterative processes. *SIAM Rev.* **30,** 375 (1988).
18. R. Seydel, *From Equilibrium to Chaos: Practical Bifurcation and Stability Analysis* (Elsevier, Amsterdam, 1988).
19. J. P. Boyd, *Chebyshev and Fourier Spectral Methods* (Springer-Verlag, Heidelberg, 1989).
20. R. E. Bank and T. F. Chan, *SIAM J. Stat. Sci. Comput.* **7,** 540 (1986).